Electronic Supplementary Material (ESI) for Nanoscale.

Extracellular vesicles from adipose stromal cells combined with a thermoresponsive hydrogel prevent esophageal stricture after extensive endoscopic submucosal dissection in a porcine model

Elise Coffin[1], Alice Grangier[2], Guillaume Perrod[1], Max Piffoux[2], Iris Marangon[2], Imane Boucenna[2], Arthur Berger[1], Leila M'Harzi[3], Jessica Assouline[4], Thierry Lecomte[5], Anna Chipont[6], Coralie Guérin[6], Florence Gazeau[2], Claire Wilhelm[2], Christophe Cellier[7], Olivier Clément[8], Amanda Karine Andriola Silva[2†*], Gabriel Rahmi[1,7†*]

[1] Laboratoire Imagerie de l'Angiogénèse, Plateforme d'Imagerie du Petit Animal, PARCC, INSERM U970, Laboratoire de Recherches Biochirugicales (Fondation Carpentier), Université de Paris, 56 rue Leblanc, 75015, Paris, France
[2] Laboratoire Matière et Systèmes Complexes (MSC), Université de Paris, UMR 7057 CNRS, 75205 Paris cedex 13, France
[3] Department of Surgery, Hôpital Européen Georges Pompidou, Assistance Publique des Hôpitaux de Paris, Université de Paris, 20 rue Leblanc 75015
[4] Departement of Radiology, Hôpital Saint Louis, Assistance Publique des Hôpitaux de Paris, Université de Paris, 1 Avenue Claude Vellefaux, 75010 Paris
[5] CIRE Plateform, UMR 0085, Physiologie de la Reproduction et des comportements, INRA, Centre Val De Loire, 37380 Nouzilly
[6] Cytometry Unit, Institut Curie, Paris, France
[7] Gastro-Enteroloy and Endoscopy Department, Hôpital Européen Georges Pompidou, Assistance Publique des Hôpitaux de Paris, Université de Paris, 20 rue Leblanc 75015
[8] Department of Radiology, Hôpital Européen Georges Pompidou, Assistance Publique des Hôpitaux de Paris, Université de Paris, 20 rue Leblanc 75015

† These authors equally contributed to this work.

* Correspondence: amanda.silva@univ-paris-diderot.fr, gabriel.rahmi@aphp.fr

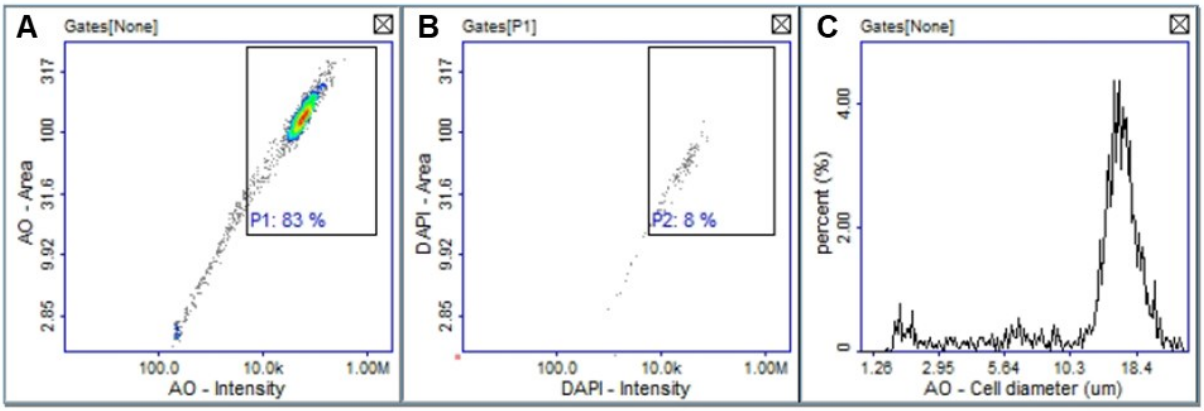

Supplementary Figure 1: Nucleocounter NC-200 analysis of ADSCs cultured in T-flasks based on double staining using acridine range (AO, panel A) and DAPI (panel B). Cell diameter was determined from AO analysis (C).

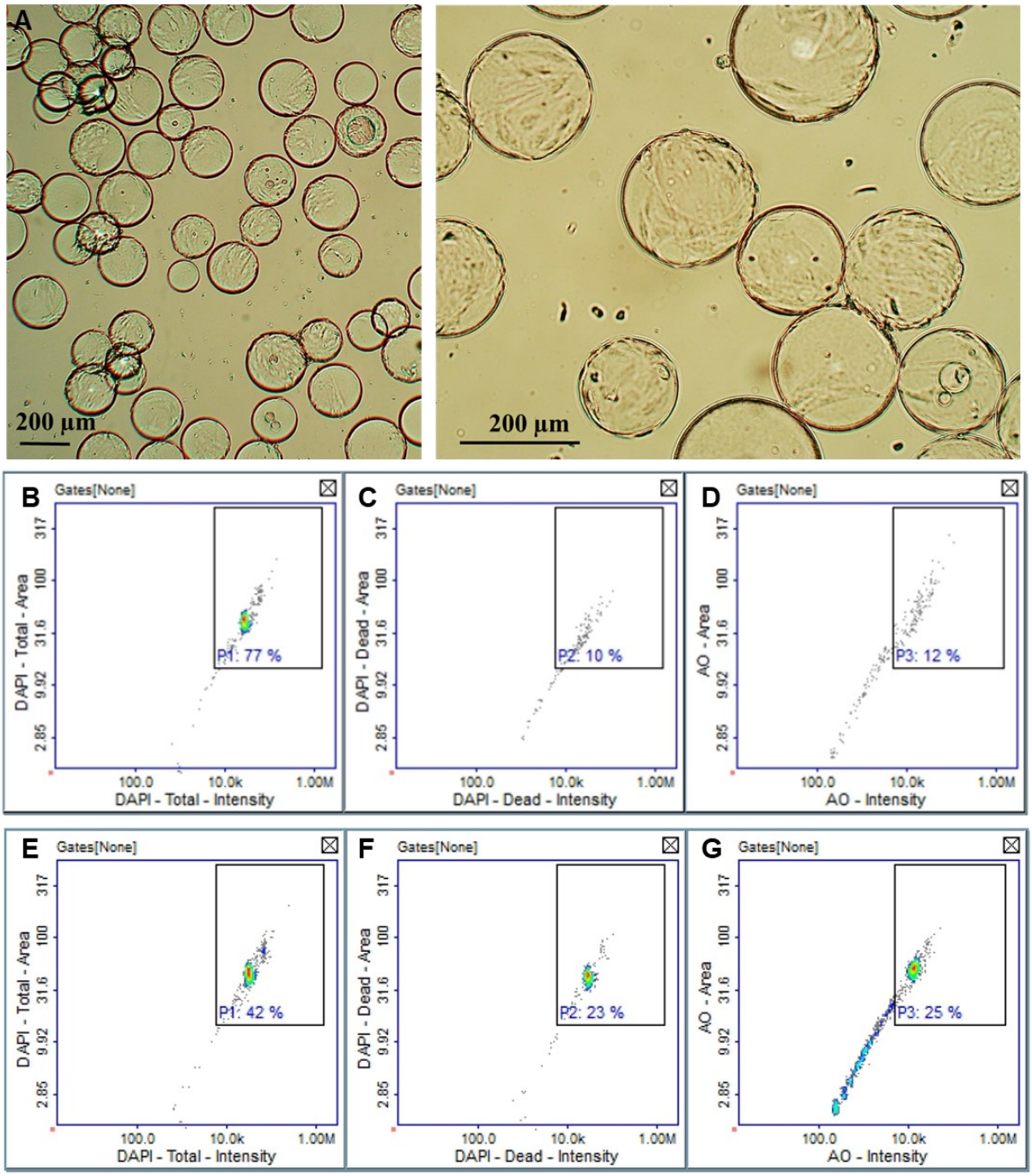

Supplementary Figure 2: Optical microsocopy images of ADSCs culture on Cytodex 3 beads in spinner flask bioreactors (A). Nucleocounter NC-200 analysis for ADSCs cultured in beads before EV production protocol by turbulence. The analysis was carried out by the "reagent A + B protocol" according to the supplier's instructions. This counting is based on nucleus quantification by DAPI before (B) and after cell lysis induced by reagent A + B via a double staining using DAPI (C) and acridine orange (D) to determine the percentage of viable cells. Nucleocounter NC-200 analysis was also performed for ADSCs cultured in beads after EV production protocol by turbulence. The analysis was

also carried out by the “reagent A + B protocol” according to the supplier’s instructions based on nucleus quantification by DAPI before (E) and after cell lysis induced by reagent A + B via a double staining using DAPI (F) and acridine orange (G) to determine the percentage of viable cells.

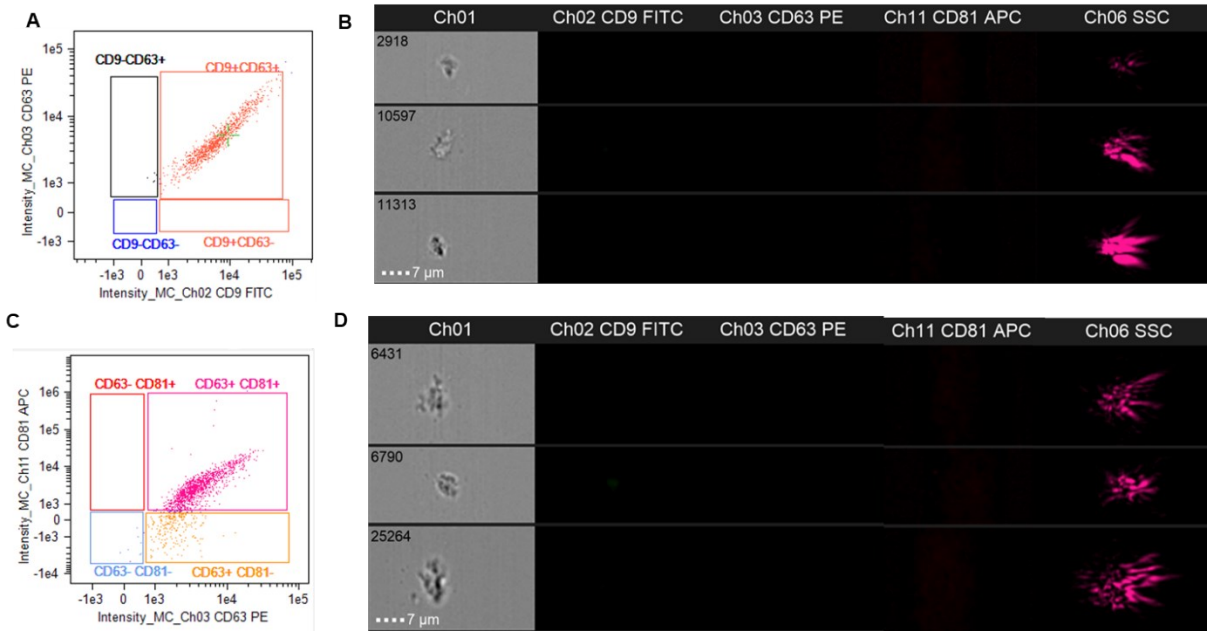

Supplementary Figure 3: AB analysis by multispectral imaging flow cytometry. The events in the AB gate for the SSC versus CD81 APC fluorescence intensity were plotted for CD63 PE versus CD9 FITC intensities to investigate, single, double and triple positiveness (A). Images acquired for single ABs detected in the triple CD9, CD63 and CD81 positive gate showed bright field and dark field signals, as expected, but no signal was detected in the green FITC channel for CD9, in the yellow PE channel for CD63 nor in the red APC channel for CD81(B). The events in the AB gate for the SSC versus CD9 FITC fluorescence intensity were plotted for CD81 versus CD63 PE fluorescence intensities to investigate single, double and triple positiveness (C). Images acquired for single ABs detected in the triple CD9, CD63 and CD81 positive gate showed bright field and dark field signals, as expected, but no signal was detected in the green FITC channel for CD9, in the yellow PE channel for CD63 nor in the red APC channel for CD81 (D).

Supplementary Table 1: Nucleo counter NC-200 analysis report table for ADSCs cultured in T-flasks based on double staining using acridine range and DAPI to determine the percentage of viable cells. Cell diameter was determined from acridine orange analysis.

Viability (%)	92.5
Live (cells/ml)	8.52E5
Dead (cells/ml)	6.89E4
Total (cells/ml)	9.21E5
Estimated cell diameter (um)	16.0
Cell diameter standard deviation (um)	9.3
(%) of cells in aggregates with five or more cells	1

Supplementary Table 2: Nucleo counter NC-200 analysis report table for ADSCs cultured in beads. The analysis was carried out by the "reagent A + B protocol" according to the supplier's instructions. This counting is based on nucleus quantification before and after cell lysis induced by reagent A + B via a double staining using acridine orange and DAPI to determine the percentage of viable cells. Cell diameter was determined from acridine orange analysis. However, it is not relevant for the "reagent A + B protocol" as only nuclei are analyzed (rather them the whole cell).

Viability (%)	94.4
Live cells (cells/ml)	1.72E6
Dead cells (cells/ml)	1.02E5
Total (cells/ml)	1.82E6
Estimated cell diameter (um)	10.5
Cell diameter standard deviation (um)	9.7

Supplementary Table 3: Nucleo counter NC-200 analysis report table for ADSCs cultured in beads after EV production protocol by turbulence. The analysis was carried out by the "reagent A + B protocol" according to the supplier's instructions. This counting is based on nucleus quantification before and after cell lysis induced by reagent A + B via a double staining using acridine orange and DAPI to determine the percentage of viable cells. Cell diameter was determined from acridine orange analysis. However, it is not relevant for the "reagent A + B protocol" as only nuclei are analyzed (rather them the whole cell).

Viability (%)	81.7
Live cells (cells/ml)	1.71E6
Dead cells (cells/ml)	3.83E5
Total (cells/ml)	2.09E6
Estimated cell diameter (um)	13.7
Cell diameter standard deviation (um)	6.9

Supplementary Table 4. Histological evaluation of the esophageal stricture for control, gel and EVs + gel groups.

	Control (n=6)	Gel (n=6)	EVs + gel (n=6)	p*
Maximum thickness of the fibrosis (mm)	2.4 ± 0.84	2.03 ± 1.43	1.85 ± 1.41	0.55
Length of the muscular mucosae (mm)	2.81 ± 4.42	6.78 ± 4.29	11.19 ± 2.54	0.0036
Maximum length of the absence of epithelium (mm)	2.7± 4.14	1.15±1.44	1.86 ±2.24	0.86